Clinical Imaging 53 (2019) 186–190

Contents lists available at ScienceDirect

Clinical Imaging

journal homepage: www.elsevier.com/locate/clinimag

Pediatric Radiology

A quantitative image analysis using MRI for diagnosis of biliary atresia

Dao Chen Lin[a,b,c], Kun Yu Wu[d], Fang Ju Sun[e,f], Chun Chao Huang[e,g,h], Tung Hsin Wu[i], Shin Lin Shih[g,j], Pei Shan Tsai[e,h,g,*]

[a] Department of Radiology, Taipei Veterans General Hospital, Taipei City 11217, Taiwan, ROC
[b] Division of Endocrine and Metabolism, Department of Medicine, Taipei Veterans General Hospital, Taipei City 11217, Taiwan, ROC
[c] School of Medicine, National Yang-Ming University, Taipei City 11221, Taiwan, ROC
[d] Department of Medical Imaging, Chi Mei Medical Center, Tainan City 71004, Taiwan, ROC
[e] Mackay Junior College of Medicine, Nursing, and Management, Taipei City 11260, Taiwan, ROC
[f] Department of Medical Research, MacKay Memorial Hospital, Tamsui Branch, New Taipei City 25160, Taiwan, ROC
[g] Department of Radiology, MacKay Memorial Hospital, Taipei City 10449, Taiwan, ROC
[h] Department of Medicine, Mackay Medical College, New Taipei City 25245, Taiwan, ROC
[i] Department of Biomedical Imaging and Radiological Sciences, National Yang-Ming University, Taipei City 11221, Taiwan, ROC
[j] Department of Radiology, Taipei Medical University, Taipei City 11031, Taiwan, ROC

ARTICLE INFO

Keywords:
Biliary atresia
Extrahepatic bile duct
Idiopathic neonatal hepatitis
Magnetic resonance imaging

ABSTRACT

Purpose: Biliary atresia is a life-threatening disease that needs early diagnosis and management. Recently, MRI images have been used for the diagnosis of biliary atresia with improved accuracy of diagnosis when other imaging modalities such as ultrasonography are equivocal. This study aimed to evaluate the juxta-hilar extrahepatic biliary tree using MRI images to determine a quantitative value for diagnosing biliary atresia.

Materials and methods: This retrospective study was approved by the Ethical Committee at Mackey Memorial Hospital (IRB Number: 15MMHIS149e). Between January 2010 and December 2015, twenty-five patients with surgically confirmed biliary atresia were enrolled (age 18–65 days). Another 25 patients with clinically or surgically diagnosed idiopathic neonatal hepatitis (age 6–64 days) and 20 patients with non-hepatobiliary disease (age 6–65 days) were considered control group and normal subjects, respectively. The diameter of the enlarged, T2-hyperintense structure was measured using MRI images by two radiologists both blinded. The cut-off value for a biliary atresia diagnosis was obtained by area under the curve analysis.

Results: The diameter of the T2-hyperintense structure at porta hepatis in biliary atresia (4.79 ± 1.14 mm) is larger than in idiopathic neonatal hepatitis (1.72 ± 0.42 mm) or in non-hepatobiliary disease (1.72 ± 0.35 mm) ($p < 0.05$). The optimum cut-off value for diagnosing biliary atresia was 3.1 mm with 98% sensitivity and 98% specificity.

Conclusion: The value of the enlarged, T2-hyperintense structure measured on MRI images was significantly increased in biliary atresia and may be useful in diagnosing biliary atresia.

1. Introduction

Biliary atresia (BA) is an inflammatory process with unknown etiology characterized by progressive fibrous-obliteration of the intrahepatic and extrahepatic biliary tree, resulting in cholestasis and secondary hepatic fibrosis [1]. BA affects 1/10,000 to1/20,000 live births globally. Asian infants have a higher incidence (Japan, 0.8–1.1/10,000; Taiwan, 2/10,000) than those in the western world (Europe and North America have lower incidences of 0.6–0.8/10,000) [2–4]. If left untreated, BA progresses to liver cirrhosis, hepatic failure, and death within a few years of life [5]. Therefore, it is the most common indication for pediatric liver transplantation. Since Kasai and Suzuki introduced hepatic portoenterostomy for the treatment of BA in 1951 [6], the prognosis has improved in most affected patients [7]. The age at which this operation performed is the main statistical determinant of successful surgery, and it is generally accepted that the Kasai operation is more successful in children younger than 60 days of age [8–11]. Therefore, early identification and intervention are necessary for the best outcome. However, early identification remains challenging [12].

Until now, ultrasonography (sensitivity and specificity are 50% and 82.85% respectively; the sensitivity, specificity, and positive predictive value of ultrasonographic triangular cord sign only are 80%, 98%, and

* Corresponding author at: Department of Radiology, MacKay Memorial Hospital, No. 92, Sec. 2, Chung-Shan N. Rd., Taipei City 10449, Taiwan, ROC.
E-mail address: purify.5372@mmh.org.tw (P.S. Tsai).

https://doi.org/10.1016/j.clinimag.2018.10.001
Received 14 May 2018; Received in revised form 17 September 2018; Accepted 1 October 2018

Table 1
MR acquisition parameters and sequences.

	Axial T1WI (in phase)	Axial T1WI (out phase)	Axial SSH-TSE T2WI	Axial SSH-TSE T2WI + F/S	Coronal SSH-TSE T2WI + F/S	MRCP
Repetion time/Echo time (ms) (TR/TE)	10/2.3	10/3.5	2100/80	2400/70	4200/90	1850/700
Flip angle (degree)	15	15	90	90	90	90
Section thickness (mm)/Gap	3/0.5	3/0.5	3/0.5	3/0.5	3/0.5	3/0.5
FOV (mm)	220	220	220	220	240	160
Matrix	388 × 266	412 × 255	528 × 345	528 × 351	312 × 375	176 × 177
Duration (min)	2.5	2.5	1.5	2	1.5	2.5

Note: FOV = field-of-view; WI = weighted image; SSH-TSE = single-shot turbo fast spin echo sequences on Philips magnetic machine.

94%, respectively [13]) and hepatobiliary scintigraphy with 99mTc-DISIDA (Technetium-99m-Diisopropyliminodiacetic Acid; sensitivity and specificity are 88.24% and 45.71% respectively) are most commonly performed clinically for diagnosing BA [14,15]. However, recently, magnetic resonance imaging (MRI) with magnetic resonance cholangiopancreatography (MRCP) has become a widely accepted, non-invasive method for evaluating extrahepatic biliary system with good tissue contrast, is free of ionizing radiation, with a sensitivity of 90%–100% [12,16,17], an accuracy of 71%–100% [12,16,18], but a low specificity [12]. Situations such as biliary plug syndrome or breast feeding can impede bile secretion causing poor visualization of the extrahepatic biliary tree, thus resulting in a false diagnosis of BA on MRI with MRCP [12].

In clinical practice, we found the isolated ultrasonographic triangular cord sign having lower sensitivity than those reported and may not be useful for BA diagnosis in our experience. Moreover, we had observed an enlarged T2-hyperintense structure at porta hepatis on MRI in BA infants but not in patients with cholestatic jaundice, who were finally diagnosed as having idiopathic neonatal hepatitis (INH).

The aim of our study was to analyze the enlarged, T2-hyperintense structure at porta hepatis on MRI in BA patients to provide a quantitative value facilitating both the sensitivity and specificity in investigating BA children, particularly when their ultrasonographic or scintigraphic findings are non-conclusive.

2. Methods and materials

2.1. Patients

This retrospective study was approved by the Ethical Committee at Mackey Memorial Hospital (IRB Number: 15MMHIS149e).

Between January 2010 and December 2015, 25 histopathologically proved cases of infants with BA (range 18–65 days) who received MRI prior to Kasai operation were enrolled and their MRI were reviewed regarding the juxta-hilar tract abnormality. During the same period, 25 infants presenting with symptoms of cholestatic jaundice and receiving MRI for etiology diagnosis with final confirmation of idiopathic neonatal hepatitis (INH) were considered as the control group (age range 6–64 days). In addition, another 20 infants (age range 6–65 days) underwent MRI for non-hepatobiliary disorders and served as the normal subject (NS) group within the study. All patients with BA and INH were evaluated using abdominal ultrasonography a week prior to MRI examination. We also obtained the age, sex, and biochemical data of liver function in BA or INH groups at the time of initial diagnosis.

2.2. Ultrasonography imaging criteria for BA diagnosis

All the infants were NPO at least 4–6 h before ultrasonography examination. The ultrasonographic criteria used by pediatrician and pediatric radiologist included the triangular cord sign, a thickened, echogenic area anterior to the right intrahepatic portal vein (> 4 mm in thickness) [13] and the so-called gallbladder ghost triad, atretic gallbladder length (< 19 mm from outer-to-outer wall), irregular or lobulated gallbladder contour, and lack of smooth/complete echogenic mucosal lining with an indistinct wall [19].

2.3. Protocol, data collection, and images analysis of MRI

All patients underwent MRI examinations with 3.0-T units (Achieva 3.0 T X-series, Philips software version of Release 3.2; Philips Medical Systems Nederland B.V, Veenpluis 4-6, 5684 PC Best, The Netherlands) with a 32-channel phased-arrayed cardiac coil. MRI sequences include axial and coronal, free breathing T1-weighted images, single-shot turbo spin-echo (SSH-TSE or SSTSE) T2-weighted images with or without fat suppression, and coronal single-shot, T2-weighted MRCP. The patients were given chloral hydrate by oral administration at a dose of 40 mg/kg body weight 20–30 min before receiving the MRI examination, if necessary. No contrast agents were given. Detailed MRI parameters are listed in Table 1.

The MRI at the level of the hepatic hilum before reaching the liver, known as porta hepatis (Fig. 1), was obtained based on coronal and axial, non-breath-hold, single-shot turbo spin-echo T2-weighted imaging sequences with/without fat suppression as measurement reference; analysis of the enlarged T2-hyperintense structure (labeled as extrahepatic biliary duct, EHBD) at porta hepatis was based on the coronal

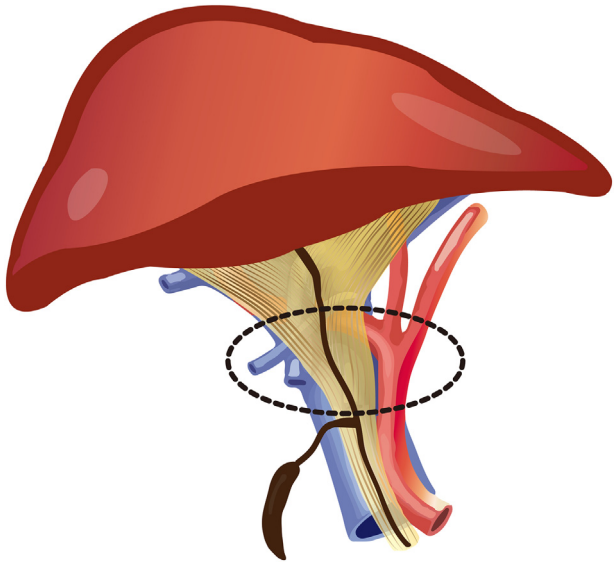

Fig. 1. Schematic figure of the structures at porta hepatis in BA patient. Blue: main portal vein; Red: proper hepatic artery; Brown structures: fibro-occlusive bile duct with surrounding fibrosis and atretic gallbladder; Dotted black circle: level where T2-weighted hyperintense structure and portal vein we measured on MRI.

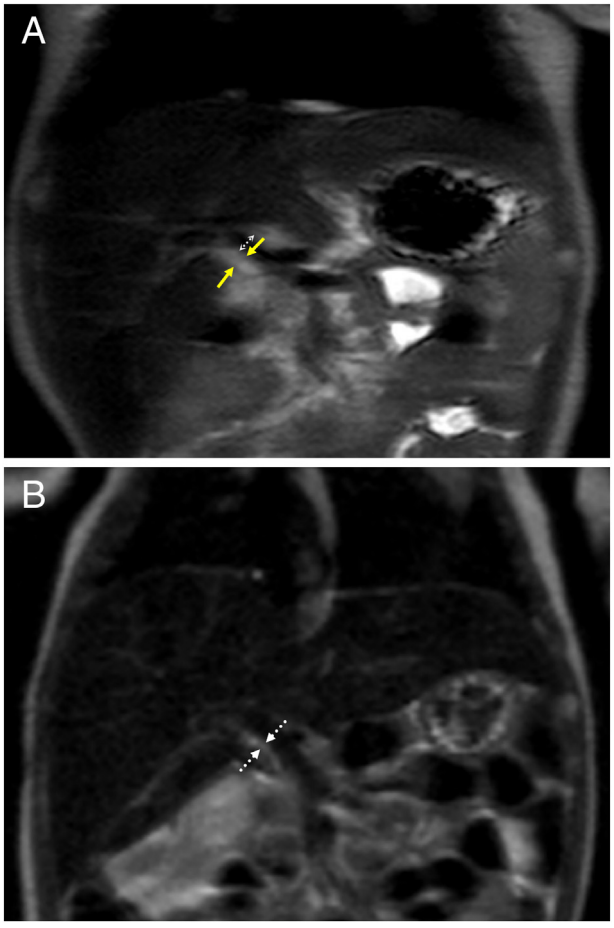

Fig. 2. MRI of extrahepatic bile duct and the accompanying main portal vein beyond confluence (double-headed arrow) at the level of hepatic hilum.
(A) coronal SSH-TSE T2-weighted image shows enlarged hyper T2WI signal (yellow solid arrows) running parallel to MPV (double-headed arrow) in biliary atresia compared with (B) the extrahepatic bile duct at hilar level (dotted arrows) seen on this coronal SSH-TSE T2-weighted image (control group).

images with picture archiving and communication system (PACS) by using free-hand measuring tool (Fig. 2A and B). The diameter of accompanied main portal vein (MPV) in the same region was also measured in each group. These measurements were performed twice by two individual experienced pediatric radiologists (P.S.T, with 11 years of experience, and K.Y.W, with 9 years of experience) both blinded. Any inconsistency during image analysis was resolved through unanimity by discussion with a senior pediatric radiologist (S.S.L., 40 years of experience reading pediatric images). The average of the values (mean ± SD) measured by the two radiologists was selected for further analysis.

2.4. Statistical analyses

Statistical analyses were performed using by SAS 9.3. The results were presented as mean ± SD. Intraclass correlation coefficient (ICC) was used to measure interrater reliability of the two radiologists. ICCs range from −1 (100% disagreement) to 1 (100% agreement). Reliability was classified as poor (ICC < 0.5), moderate (ICC = 0.5–0.75) or excellent (ICC > 0.75). Between-group differences were assessed by *t*-test and Chi-square (for sex). The cut-off value was calculated by the area under the curve (AUCROC) with optimal sensitivity. p values < 0.05 were considered indicative of a statistically significant difference.

Table 2
Clinical characteristics of the study populations.

	BA (n = 25)	INH (n = 25)	NS (n = 20)
Age (days)	41.2 ± 13.4	40.0 ± 15.6	32.3 ± 18.4
Sex (female/male)	15/10	13/12	6/14
ALT (14–40 IU/L[a])	88.2 ± 73.1	93.6 ± 87.1	NA
AST (15–41 IU/L[a])	141.4 ± 119.1	151.2 ± 146.4	NA
Total bilirubin (0.3–1.2 mg/dL[a])	9.07 ± 4.26	8.15 ± 3.03	NA
Direct bilirubin (0.1–0.5 mg/dL[a])	4.45 ± 1.44	4.15 ± 1.93	NA
G-GT (7–50 IU/L[a])	375.5 ± 251.5*	140.6 ± 99.7*	NA

Data presented as mean ± SD, NA: not available. Note: BA = biliary atresia; INH = idiopathic neonatal hepatitis; NS = normal subjective; ALT = alanine aminotransferase; AST = aspartate aminotransferase; G-GT = r-glutamyl-transferase.
* $p < 0.05$ between BA and INH group
[a] As reference normal ranges.

3. Results

3.1. Study populations

The clinical characteristics of the three study populations are listed in Table 2. No difference for age ($p = 0.17$) and sex ($p = 0.12$) was found among the groups. Levels of alanine aminotransferase (ALT) ($p = 0.82$), aspartate aminotransferase (AST) ($p = 0.81$), total ($p = 0.37$) and direct ($p = 0.55$) bilirubin were not different between the BA and INH groups. However, the gamma-glutamyl transferase (G-GT) was significantly higher in the BA group (375.5 ± 251.5 IU/L) than in the INH group (140.6 ± 99.7 IU/L) ($p < 0.01$).

3.2. Ultrasonography for diagnosis of BA

According to the above mentioned of triangular cord sign and gallbladder ghost triad criteria, ultrasonography distinguished BA and INH in our institute with a sensitivity of 44% and 88%, specificity of 100% and 48%, positive predictive value of 100% and 63%, negative predictive value of 36% and 20%, respectively.

3.3. Reliability of image interpretation in MRI

The ICC values of T2-hyperintense structure or EHBD measurement were 0.993 in BA group ($p < 0.01$), 0.825 in INH and NS group ($p < 0.01$), and 0.989 ($p < 0.01$) in combined three groups between our two radiologists. In MPV measurement, the ICC values were 0.937 ($p < 0.01$) in BA group, 0.595 ($p < 0.05$) in INH and NS group, and 0.716 ($p < 0.01$) in combined three groups between two radiologist. Hence, the interrater reliability for measuring the value of T2-hyperintense structure and accompanied MPV at porta hepatis using MRI were excellent (ICC > 0.75) and moderate (ICC 0.5–0.75) respectively.

3.4. Measurement of the T2-hyperintense structure/EHBD and MPV at porta hepatis in BA, INH, and NS patients by MRI

The mean measured diameter of MPV were 4.35 ± 0.57 mm, 4.17 ± 0.50 mm, and 4.07 ± 0.41 mm in BA, INH, and NS groups, respectively. There was no difference in the mean measured diameter among the three groups. The mean measured values of the T2-hyperintense structure/EHBD at porta hepatis were 4.79 ± 1.14 mm, 1.72 ± 0.42 mm and 1.72 ± 0.35 mm in BA, INH and NS groups, respectively. Results for the different study populations are summarized in Table 3.

The measured value of the T2-hyperintense structure in patients with BA was significantly larger than that in patients with INH and NS ($p < 0.05$). On ROC curve analysis, the optimal cut-off value for

Table 3
MRI measurement of diameters of extra hepatic bile duct (EHBD) and main portal vein (MPV) at hepatic hilum in biliary atresia (BA), idiopathic neonatal hepatitis (INH), and normal subjects (NS).

	BA (n = 25)	INH (n = 25)	NS (n = 20)
EHBD[a] (mm)	4.79 ± 1.14*	1.72 ± 0.42*	1.72 ± 0.35*
MPV[b] (mm)	4.35 ± 0.57	4.17 ± 0.51	4.07 ± 0.41

Data presented as mean ± SD. EHBD[a] in BA represents with the area of abnormal inflammation and fibrosis containing occluded bile duct remnant. MPV[b]: main portal vein at juxta hilar region before reaching liver (portal hepatis).

* $p < 0.05$ between BA and other two groups.

Table 4
Accuracy for diagnosis of biliary atresia by different image modalities and criteria in our study.

	Triangular cord sign of ultrasound	Gallbladder ghost triad of ultrasound	Hyper T2WI signal > 3.1 mm in MRI
Sensitivity	44%	88%	98%
Specificity	100%	48%	98%

diagnosing BA was 3.1 mm with 98% sensitivity and 98% specificity using area under the curve method. The diagnostic performance by ROC curve was 0.997.

The sensitivity and specificity of ultrasonography and MRI for diagnosis of BA are summarized in Table 4.

4. Discussion

Currently, many non-invasive imaging modalities are used for diagnosing BA before invasive examinations are performed. These include ultrasonography, hepatobiliary scintigraphy with 99mTc-DISIDA and MRI with MRCP. Additionally, all of these modalities do not provide diagnostic results individually [20].Although the ultrasonographic triangular cord sign has been reported with a positive predictive value of 94% [13], Anne et al. found this sign is only helpful when the involved livers had not undergone cirrhotic change [19]. Conversely, fibrotic hepatic parenchyma can mask the ultrasonographic triangular cord sign and this has been commonly observed in clinical practice.

In recent decades, MRI with MRCP has been widely used for diagnosing BA. Previous MRI studies have shown that BA can be reliably diagnosed by non-visualization of the extrahepatic biliary tree, especially when accompanied by an atrophic or atretic gallbladder [12,16–18]. Furthermore, some conditions can impede bile secretion, such as biliary plug syndrome or breastfeeding, causing poor visualization or poor identification of the extrahepatic biliary tree, resulting in incorrect diagnosis of BA on MRI with MRCP [12].

According to Kim et al., the triangular area of high-signal intensity confined to the porta hepatis on T2-weighted MRCP is helpful in correctly diagnosing BA [21]. However, in our daily practice and experience, this imaging pattern is not identified as early as we thought and might be masked by nonspecific periportal inflammation or cirrhosis [22].Therefore, we designed this study using non-breath-hold, single shot turbo spin-echo T2-weighted sequences with/without fat suppression rather than the single-shot, T2-weighted MR cholangiography (a kind of heavily T2-weigthed sequence) used by Kim et al. as it has better signal-to-noise ratio [23], excellent imaging quality of bile duct anatomy, biliary tree anomaly and the close relationship of the accompanied MPV [24].

In our retrospective study, the use of ultrasonography for distinguishing BA from INH yielded poor results owing to low sensitivity of triangular cord sign and low specificity by gallbladder ghost triad. However, using MRI, we found an enlarged T2-hyperintense structure at the level of porta hepatis in BA which was significantly larger than that in the INH and NS groups, seemed to distinguish BA from INH more easily than ultrasonography. In our analysis, the optimal cut-off value of T2-hyperintense structure for diagnosing BA was > 3.1 mm and had good diagnostic performance (ROC curve was 0.997).

After correlating with the surgery records, the enlarged, T2-hyperintense structure at the juxta-hilar level (as known as porta hepatis) was likely caused by inflammation of fibrous and occlusive extrahepatic biliary duct which may be the extension of the echogenic tissue cranial to the intrahepatic portal vein bifurcation (the so-called triangular cord sign on ultrasonography) to porta hepatis.

There are some limitations to this study. First, this is a retrospective analysis which is susceptible to bias in patient and data selection. Second, to our knowledge, there are no widely accepted standards for the normal size of an extrahepatic biliary tree in neonates and young infants on MRI. In our study, we provide normal extrahepatic biliary duct caliber in the level of the hepatic hilum in the NS group which was smaller than that reported previously [25]. The explanations might be attributed to younger age of the patients in the NS group and non-identical measuring level of extrahepatic biliary duct. Lastly, even with recent improvement of MRI coil technology, increased acquisition speed and newer respiratory compensation techniques, the small caliber of the biliary tree, patients' movement, and poor signals can make correct diagnosis more difficult.

5. Conclusion

In brief, the value of enlarged T2-hyperitense structure at porta hepatis may be an alternative helpful quantitative measurement in MRI for diagnosis of BA particularly when ultrasonographic or other image findings are inconclusive.

Conflict of interest

All authors declare no affiliation with any organization regarding direct or indirect financial interest in the subject matter discussed in the manuscript.

Declarations of interest

None.

IRB statement

The study was approved by the Ethical Committee at the Mackey Memorial Hospital (IRB Number: 15MMHIS149e).

Funding

This research did not receive any specific grant from funding agencies in the public, commercial, or not-for-profit sectors.

References

[1] Petersen C. Pathogenesis and treatment opportunities for biliary atresia. Clin Liver Dis 2006;10:73–88.
[2] Davenport M, De Ville de Goyet J, Stringer MD, et al. Seamless management of biliary atresia in England and Wales (1999–2002). Lancet 2004;363:1354–7.
[3] Schreiber RA, Barker CC, Roberts EA, et al. Biliary atresia: the Canadian experience. J Pediatr 2007;151:659–665, 665.e1.
[4] Wada H, Muraji T, Yokoi A, et al. Insignificant seasonal and geographical variation in incidence of biliary atresia in Japan: a regional survey of over 20 years. J Pediatr Surg 2007;42:2090–2.
[5] Chiu CY, Chen PH, Chan CF, et al. Biliary atresia in preterm infants in Taiwan: a nationwide survey. J Pediatr 2013;163. [100.e1–103.e1].
[6] Kasai M, Suzuki S. A new operation for “non-correctable” biliary atresia: hepatic portoenterostomy. Shujutsu 1959;13:733–9.
[7] Ohi R, Chiba T, Endo N, et al. Long-term follow-up after surgery for patients with biliary atresia. J Pediatr Surg 1990;25:442–5.

[8] Lien TH, Chang MH, Wu JF, et al. Effects of the infant stool color card screening program on 5-year outcome of biliary atresia in Taiwan. Hepatology 2011;53:202–8.
[9] Ohi R. Surgery for biliary atresia. Liver 2001;21:175–82.
[10] Hsiao CH, Chang MH, Chen HL, et al. Universal screening for biliary atresia using an infant stool color card in Taiwan. Hepatology 2008;47:1233–40.
[11] Khalil BA, Perera MT, Mirza DF. Clinical practice: management of biliary atresia. Eur J Pediatr 2010;169:395–402.
[12] Liu B, Cai J, Xu Y, et al. Three-dimensional magnetic resonance cholangiopancreatography for the diagnosis of biliary atresia in infants and neonates. PLoS One 2014;9:e88268.
[13] Lee HJ, Lee SM, Park WH, et al. Objective criteria of triangular cord sign in biliary atresia on US scans. Radiology 2003;229:395–400.
[14] He JP, Hao Y, Wang XL, et al. Comparison of different noninvasive diagnostic methods for biliary atresia: a meta-analysis. World J Pediatr 2016;12:35–43.
[15] Imanieh MH, Dehghani SM, Bagheri MH, et al. Triangular cord sign in detection of biliary atresia: is it a valuable sign? Dig Dis Sci 2010;55:172–5.
[16] Norton KI, Glass RB, Kogan D, et al. MR cholangiography in the evaluation of neonatal cholestasis: initial results. Radiology 2002;222:687–91.
[17] Han SJ, Kim MJ, Han A, et al. Magnetic resonance cholangiography for the diagnosis of biliary atresia. J Pediatr Surg 2002;37:599–604.
[18] Jaw TS, Kuo YT, Liu GC, et al. MR cholangiography in the evaluation of neonatal cholestasis. Radiology 1999;212:249–56.
[19] Tan Kendrick AP, Phua KB, Ooi BC, et al. Biliary atresia: making the diagnosis by the gallbladder ghost triad. Pediatr Radiol 2003;33:311–5.
[20] Humphrey TM, Stringer MD. Biliary atresia: US diagnosis. Radiology 2007;244:845–51.
[21] Kim MJ, Park YN, Han SJ, et al. Biliary atresia in neonates and infants: triangular area of high signal intensity in the porta hepatis at T2-weighted MR cholangiography with US and histopathologic correlation. Radiology 2000;215:395–401.
[22] Peng SS, Jeng YM, Hsu WM, et al. Hepatic ADC map asan adjunct to conventional abdominal MRI to evaluate hepatic fibrotic and clinical cirrhotic severity in biliary atresia patients. Eur Radiol 2015;25:2992–3002.
[23] Vitellas KM, Keogan MT, Spritzer CE, et al. MR cholangiography of bile and pancreatic duct abnormalities with emphasis on single-shot FSE technique. Radio Graph 2000;20:939–57.
[24] Delaney L, Applegate KE, Karmazyn B, et al. MR cholangiopancreatography in children: feasibility, safety, and initial experience. Pediatr Radiol 2008;38:64–75.
[25] Gwal K, Bedoya MA, Patel N, et al. Reference values of MRI measurements of the common bile duct and pancreatic duct in children. Pediatr Radiol 2015;45:1153–9.